Texture evolution in Mg-Al and Mg-RE alloy during hot extrusion

Jie Dong [a], Jie Sun [a], Li Jin [a], Zhenyan Zhang [a] and Wenjiang Ding [a, b]

[a] *National Engineering Research Center of Light Alloy Net Forming, Shanghai Jiaotong University, Shanghai 200240, PR China*
[b] *Key State Laboratory of Metal Matrix Composite, Shanghai Jiaotong University, Shanghai 200240, PR China*

Abstract

The application of Mg alloys is greatly restricted because of their poor plasticity, which is closely related with the texture formed during hot forming. In this paper, the texture evolutions in Mg-Al and Mg-RE alloy during extrusion have been investigated. The results suggested that the texture of Mg alloy extrusion bar and tubes could be weakened by Ce addition with small content, but it does not work when Al is also exists. Thus, the Mg-RE alloys exhibit much higher tensile elongation and good yield symmetry. The mechanism of texture weakening by RE addition is due to the solute effect, which could surpass the twinning and activated non-basal slip.

Keywords: Texture, Mg-Al alloy, Mg-RE alloy, extrusion

1. Introduction

Deformation structures produced during high temperature extrusion of Mg rods recrystallize to produce a ring fiber texture with the c-axes of the grains perpendicular to the extrusion direction (ED) [1-2]. Such extrusions exhibit poor ductility and strong anisotropy [3] in their mechanical properties. Texture weakening or randomization is a desirable approach to get high ductility Mg alloys and a number of cases of weak or non-basal textures have been reported recently for Mg alloy sheets and extrusions [3-7]. Various authors have suggested that texture could be weakened via dynamical recrystallization during the processing with addition of Y, Ce and other rare earth elements. Mishra et. al [5] have shown that tensile ductility of extruded Mg-0.2wt% Ce is significantly enhanced due to texture randomization where the basal planes get oriented at 40~50° to the extrusion direction (ED) in the recrystallized microstructure.

Texture weakening in Mg alloy have been associated with various phenomena, including abnormal grain growth [8-9], particle-stimulated nucleation (PSN) [3, 6], particle pinning [10], solute drag [4], dynamic strain aging [11] and heterogeneous deformation leading to ease of shear band formation [6-7]. To clarify the effect of RE-element addition on the recrystallization texture after extrusion and to optimize the processing conditions for producing random texture in the Mg alloy extrusions, the microstructures of Mg-Ce and Mg-Al-Ce alloy tubes or rods have been investigated in this study. The approach for developing wrought Mg alloys with texture randomization and strengthening via alloying is discussed on the basis of the results.

2. Experimental

The materials studied in this work include nominally pure Mg (baseline), Mg-Ce, Mg-Al, and Mg-Al-Ce alloys. Unalloyed Mg and Mg alloy melts of about 100kg were prepared using commercially pure Mg ingots, pure aluminum and Mg-20%Ce master alloy in a steel crucible with SF6/CO2 protective cover gas. Billets of 75mm diameter and 230mm length were cast at about 700ºC into a permanent mold. The billets were preheated to 400 ºC for two hours and extruded in a Wellman Enefco™ 500-ton multipurpose vertical hydraulic press fitted with a circular die. Solid rods, approximately 15mm in diameter corresponding to an extrusion ratio (ER) of 25 were extruded using boron nitride lubricant at a billet speed of 10mm s^{-1} and air cooled.

Metallographic samples were prepared by standard methods, and the polished samples were etched in a solution containing 20ml glacial acetic acid, 50ml picric acid, 10ml methanol and 10ml deionized water. The polished samples were examined by the scanning electron microscope (SEM) and electron backscattered diffraction (EBSD) in a LEO™ 1450 SEM operating at 20kV fitted with a TSL™ EBSD camera [5]. The compositions of the particles in the Mg alloys were analyzed by electron probe microanalysis (EPMA). EBSD scans were obtained using beam step size of 2mm and a camera length of 18cm from an area approximately 1mm x 1mm and at least three different scans from the same sample were collected to ascertain the repeatability of the results. The inverse pole figure (IPF) map, image quality map with the twin boundaries outlined, and the (0001), (10-10), and (1-210) pole figures were processed with TSL OIM commercial software.

3. Results

The original microstructure including of AZ31 and AM30 alloy tubes are showed in Fig. 1, the IPF map in Fig. 1a and 1b show crystallization occurred during extrusion and the grain boundaries among majority grains are high angle grain boundaries with their misorientation higher than 15°, and average grain size is 50mm for AZ31 and 30mm for AM30. Pole figure shows ring basal texture with their c-axes perpendicular to extrusion direction(ED) in the two samples, but the majority grain orientations can be divided into two groups: one with their c-axes approximately parallel to the radial direction (Called the RD component) and the other with their c-axes approximately parallel to the tangential direction (Called the TD component), which is the typical extruded tube texture. And the max texture intensity is 5.704 and 5.051 for AZ31 and AM30, respectively.

The EBSD inverse pole figure (IPF) maps and corresponding (0001), (10-10), and (11-20) texture plots from as-extruded tubes of Mg-0.2Ce are shown in Figures 2(a) and (b). The differences in the texture between Mg-0.2Ce and AZ31, AM30 are evident from these figures. In the case of the Mg-0.2Ce tubes, the c-axes of the grains are not normal to the extrusion axis but make an angle about 45° to the extrusion axis, as is evident from the texture plot in Figure 2(b). This is similar to what has been reported in Mg-0.2Ce rods [10]. As the RD component shows clearly, the TD component seems to be very weak. Besides, the tensile curve of as-extruded tubes of Mg-0.2Ce tube is shown in Fig.2(c) compared with that of pure-Mg. It can be seen clearly that with the addition of 0.2%Ce the ductility enhances a lot.

With the addition of Ce and Al, the formability of the tubes and the macroscope of the tube are enhanced as showed in Fig. 3a. However, the deflection of the main texture seen in Mg-0.2Ce alloy did not occur in the case of Mg-3Al-0.5Ce alloy tube which can be seen in Fig.3 (b). The texture of Mg-3Al-0.5Ce is similar to that of AZ31. The tension and compression mechanical property are shown in Fig.3 (c). It can be seen that the strength of alloy increased a lot compared with Mg-0.2Ce but also exhibited the obvious yield asymmetry which can be seen widely in textured Mg alloys. And the elongation of Mg-3Al-0.5Ce alloy is about 20% which is lower than that of Mg-0.2Ce alloy.

The effects of RE addition on the texture of extrusion rod were also investigated in this study. The texture of pure-Mg, Mg-0.2Ce and Mg-3Al-0.2Ce alloy rods are shown in Fig.4 in a same reference frame to get a flagrant contrast. For the Mg-0.2%Ce alloy, the texture altered from typical

ring basal texture as showed in Fig. 4a, but for the Mg-3%Al-0.2%Ce alloy rod, the texture is similar with that in AZ31 or pure Mg rod.

Fig. 5 shows the backscattered electron micrographs along with the electron probe composition maps. The samples were taken from the longitudinal section (extrusion axis parallel to the sample plane). The results show that some particles in Mg-3%Al-0.2%Ce alloy have a composition close to $Mg_{17}Al_{12}$ phase an others with a composition close to $Al_{11}Ce_3$ are seen aligned along the ED [13]. By contrast, small intermetallic $Mg_{12}Ce$ phase particles [12] are distributed homogeneously in the Mg-0.2Ce alloy. In addition, the electron probe maps of individual element compositions in Fig. 5 suggest that, in the Mg-0.2Ce, the solute Ce is distributed in the matrix while there is no measurable solute Ce present in the matrix of the Mg-3%Al-0.2%Ce sample.

4. Discussion

Deformed Mg acquires a preferred orientation or texture because deformation occurs on the most favorably orientated slip or twinning systems that reorient the grains [14]. The ring basal texture and rolling basal texture are almost universal in extruded Mg rod [2, 4, 15] and rolled Mg sheet [15-17], respectively, because of the basal slip and {10-12}extension twinning [18-19] dominating the deformation process. Fig. 6 shows IPF and PF maps of AZ31 tube compressed at room temperature to true strain of: (a) 0.01 (b)0.09 (C) 0.18. The figure shows that the {10-12} extension twinning resulted in the orientation altered during compression, in which the [0001] of twins is parallel to compression axis. That is the reason why the textures in AZ31 and AM30 tubes show TD and RD component as showed in Fig. 1. These textures are retained through the recrystallization stage. In this study, the Mg-0.2 wt.% Ce alloy tube and rod exhibited non-basal texture after hot extrusion, e.g. the basal poles were rotated ~45° towards the extrusion direction (ED). A postulate is an idea that the deformation mechanism in Mg-0.2 wt.% Ce is different from that in pure Mg and AZ31, e.g. there is few twinning and more non-basal slip in Mg-Ce alloy system.

In earlier studies of relationship between particle simulated nucleation (PSN) and recrystallization texture in Mg alloys, the weakening of the texture of WE54 alloy[3, 6] with 4wt% RE was ascribed to particle simulated nucleation or PSN. More recent studies [4] of Mg-1 wt.% Y alloy have showed significant texture-randomization even though this alloy is expected to contain very few particles [20]. Increasing the Mn content (i.e. particle) in AZ31 does not lead to changes in the sheet texture [21]. PSN alone cannot explain the different texture in AZ31 and ME10 alloy although both alloys contain particles [22]. In this study, weak or non-basal texture in the Mg alloy with 0.2 wt.% Ce, addition, and typical ring basal texture in the Mg-3 wt.%-0.2 wt.% Ce alloys are observed. Microprobe analysis for those samples (Fig. 5) indicated that there are many particles in Mg-0.2 wt.% Ce and Mg-3 wt.%Al-0.2 wt.% Ce alloys. The results suggest that particles are not necessary for the texture randomization in magnesium.

Comparing the solute (Ce and Al) distribution in the Mg-0.2 wt.% Ce and Mg-3 wt.% Al-0.2 wt.% Ce (Fig. 5), Solute Ce is distributed in the magnesium matrix in Mg-0.2 wt.% Ce alloy, but Ce is exhausted by the $Al_{11}Ce_3$ particles and no solute Ce is found in the matrix in Mg-3 wt.%-0.2 wt.% Ce alloy. The difference suggests that Ce solute in the magnesium may be necessary for the texture randomization for the Mg-Ce alloys. Al solute does not affect the texture according to the microstructure in AZ31 alloy presented in Fig.1. The above results point to the fact that Mg alloys, which are solute-strengthened by Al addition will not benefit from texture modification for ductility enhancement but such addition can influence grain refinement in lean Al alloys when Al content is below solubility limit. Concurrent strengthening and texture modification in Mg alloys have been reported in Mg-Zn-Ce alloys where Zn-Ce intermetallics have not been reported [7, 24].

Solute drag is known to influence both the grain boundary mobility of different grain boundary or ientations [14] and the recrystallization kinetics [23]. In this study, the grain structures in Fig.2 show more equiaxed grains and higher grain aspect ratio in the alloys with Ce in solution. This is consistent with Ce solutes influencing the boundary mobility due to solute drag to influence texture. Al solutes in magnesium do not affect the texture evolution during the hot extrusion as solute drag effect could be

absent at the temperature/strain rate combination present during extrusion. In Mg-3 wt.%-0.2 wt.% Ce alloy, the Ce and Al are tied up in $Al_{11}Ce_3$ phase and no Ce solute is present in the alloy, leading to th e ring basal texture. The solute drag effect in Mg-RE alloy is discussed broadly however how the solut e RE works on the deformation modes or recrystallization behavior is still confusion.

5. Summary

The texture evolutions in Mg-Al and Mg-RE alloy during extrusion have been investigated. The results suggested that the texture of Mg alloy extrusion bar and tubes could be weakened by Ce addition with small content, but it does not work when Al also exists. Thus, the Mg-RE alloys exhibit much higher tensile elongation and good yield symmetry. The mechanism of texture weakening by RE addition is due to the solute effect, which could surpass the twinning and activated non-basal slip.

ACKNOWLEDGMENTS

This work was supported by National Natural Sciences Foundation of China (Grant Nos. 50901044 and 51271118) and Shanghai Rising-Star Program (B type) (Grant No. 12QB1403300)

References

[1] A. Styczynski, C. Hartig, J. Bohlen, D. Letzig, Scripta Materialia 2004, Vol. 50, pp. 943-947.
[2] L. Jiang, R. K. Mishra, A. A. Luo, A. K. Sachdev, S. Godet. Acta Materialia 2007, Vol. 55, pp. 3899-3910.
[3] E. A. Ball, P. B. Prangnell. Scripta Materialia 1994, Vol. 31, pp. 111-116.
[4] J. Bohlen, J. W. Senn, D. Letzig, S. R. Agnew, Acta Materialia 2007, Vol. 55, pp. 2101-2112.
[5] R. K. Mishra, P. R. Rao, A. K. Sachdev, A. M. Kumar, A. A. Luo. Scripta Materialia 2008, Vol. 59, pp. 562-565.
[6] L. W. F. Mackenzie, F. J. Humphreys, G. W. Lorimer.. Materials Science and Technology 2007, Vol. 3, pp. 1173-1179.
[7] L. W. F. Mackenzie, M. O. Pekguleryuz.. Scripta Materialia 2008, Vol.59, pp. 665-668.
[8] M. T. Perez-Prado, O. A. Ruano. Scripta Materialia 2003, Vol. 48, pp. 59-64.
[9] F. J. Humphreys. Acta Materialia 1997, Vol. 45, pp. 5031-5049.
[10] T. Laser, T. Ebeling, M.R. Nürnberg, D. Letzig, R. Bormann., Magnesium Technology, TMS (The Minerals, Metals & Materials Society), 2008, pp.283-288.
[11] L. Jiang, J.J. Jonas and R. Mishra, Materials Science and Engineering A, 2011 Vol. 528, pp. 6596– 6605
[12] L. L. Rokhlin. Magnesium Alloys Containing Rare Earth Metals, Published by Taylor & Francis, 2003.
[13] N.D. Saddock, A. Suzuki, K. Wu, S.C. Wildy, Y.A. Chang, T.M. Pollock, J. W. Jones, Magnesium Technology, TMS (The Minerals, Metals & Materials Society) 2005, pp. 121-126.
[14] F. J. Humphreys. Recrystallization and related annealing phenomena. Published by ELSECIER Ltd, 2004, pp. 67.
[15] Y. N. Wang, J. C. Huang. Materials Chemistry and Physics, 2003, Vol. 81, pp. 11-26.
[16] Q. Jin, S. Lim. Scripta Materialia 2006, Vol. 55, pp. 843-846.
[17] M. R. Barnett, M. D. Nave, C. J. Bettles. Materials Science and Engineering A 2004, Vol. 386, pp. 205-211.
[18] M. D. Nave, M. R. Barnett. Scripta Materialia 2004, Vol. 51, pp. 881-885.
[19] J. Bohlen, S. B. Yi, J. Swiostek, D. Letzig, H. G. Brokmeier, K. U. Kainer.. Scripta Materialia 2005, Vol. 53, pp. 259-264.
[20] S. R. Agnew, J. W. Renn, J. A. Horton, JOM, 2006, Vol. 58, pp. 62-69.

[21] T. Laser, M. R. Nürnberg, A. Janz, C. Hartig, D. Letzig, R. Schmid-Fetzer, Bormann R. Acta Materialia 2006, Vol. 54, pp. 3033-3041.
[22] N. Stanford, M. Barnett. Scripta Materialia 2008, Vol. 58, pp. 179-182.
[23] K Lücke, K Detert . Acta Metallurgica 1957, Vol. 5, pp. 628-637.
[24] A. A. Luo, R. K. Mishra, A.K. Sachdev, Scripta Materialia 64 (2011) 410 – 413

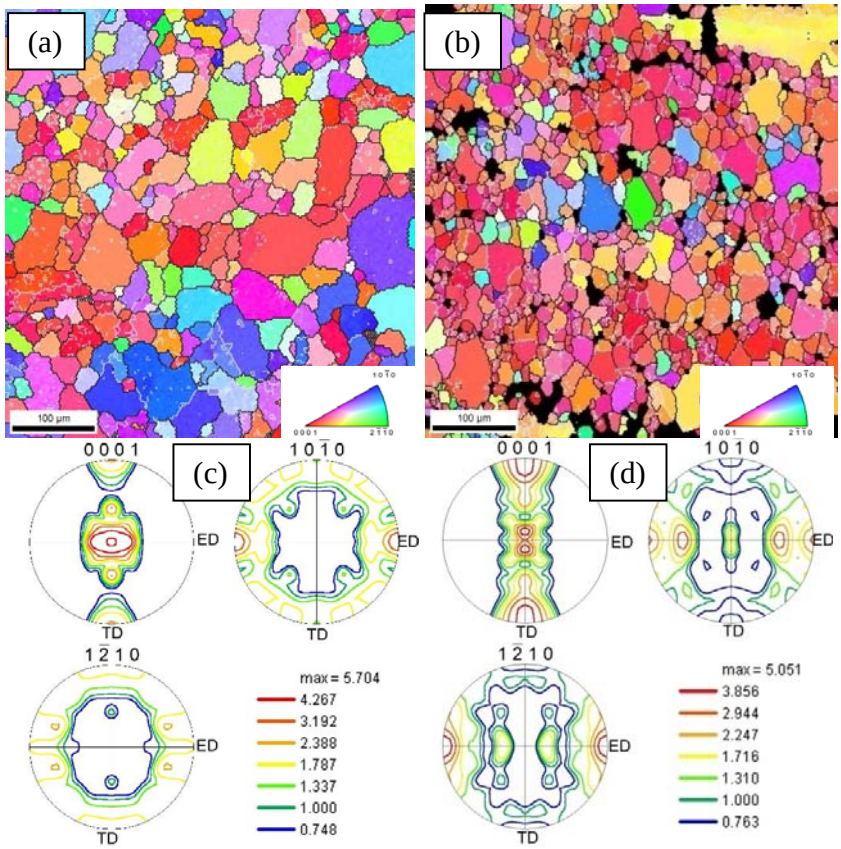

Fig.1 The microstructure and texture of the as-received AZ31and AM30 alloy tube. (a) PF map of AZ31, (b) IPF map AM30 (c) Pole figure of AZ31 (d) Pole figure of AM30.

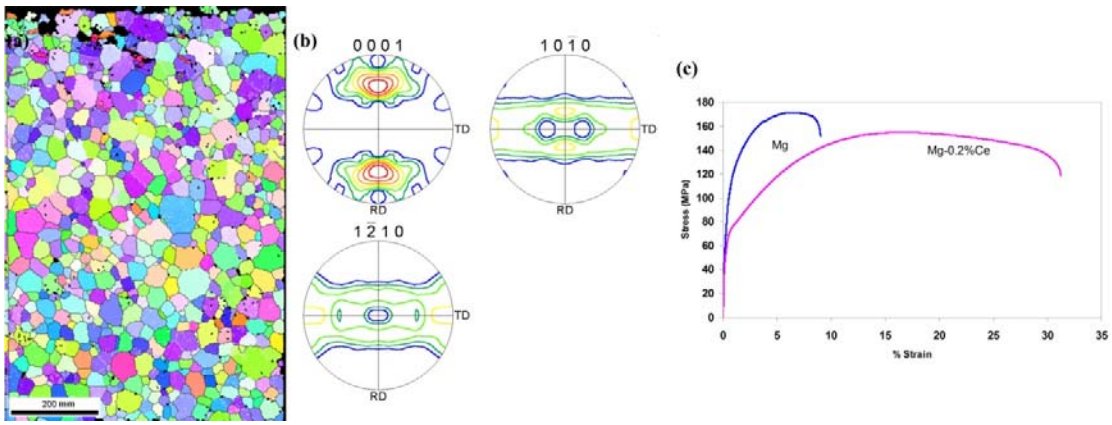

Fig.2 (a) IPF maps, (b) corresponding (0001), (10-10), and (11-20) texture plots, and (c) tensile curve of as-extruded tubes of Mg-0.2Ce tubes

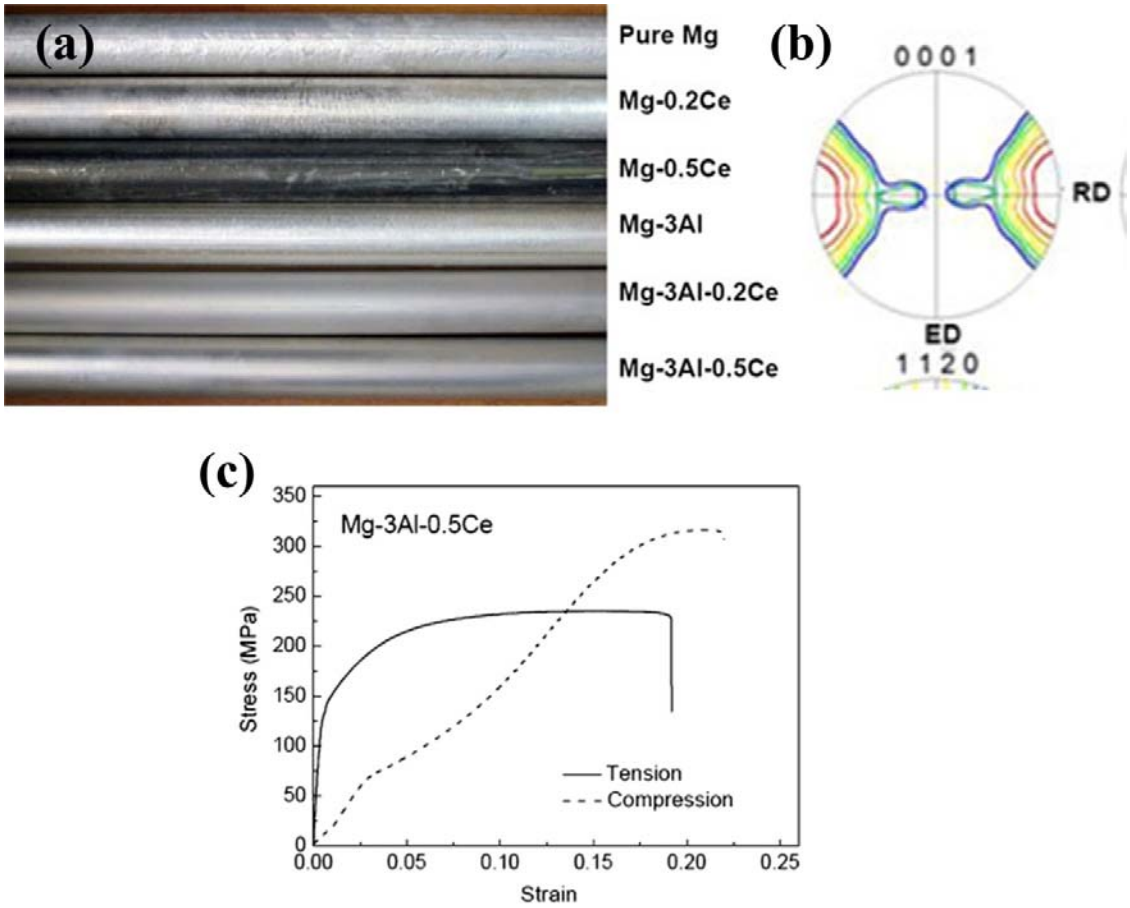

Fig. 3 Macroscope, texture and mechanical properties of Mg-Al and Mg-RE alloy tubes: (a) extruded tubes, (b) (0001) pole figure of Mg-3Al-0.5Ce alloy tube, (c) tensile and compression curve of Mg-3Al-0.5Ce alloy tube

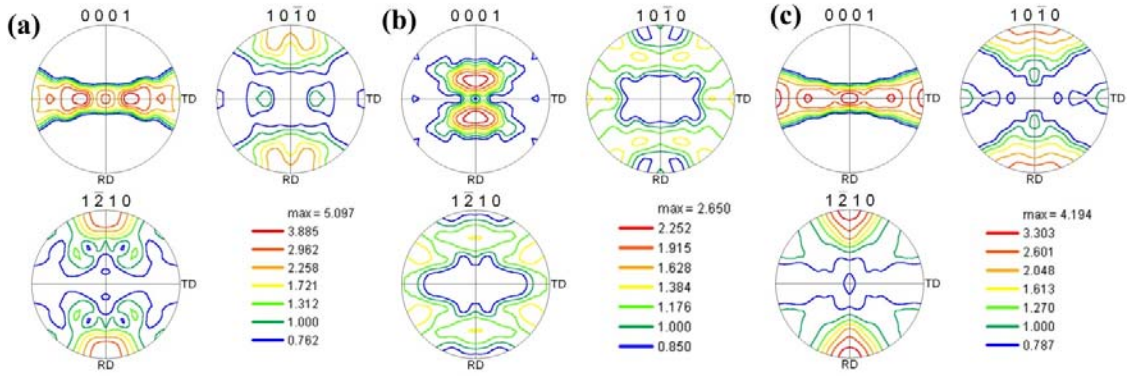

Fig. 4 (0001), (10-10) and (1-210) pole figures of Mg and alloys from the longitudinal section. TD refers to the tangential direction and ED to the extrusion direction. The sample surface normal is parallel to the radial direction: (a) unalloyed Mg, (b) Mg-0.2 wt.% Ce, (c) Mg-3 wt.% Al-0.2 wt.% Ce.

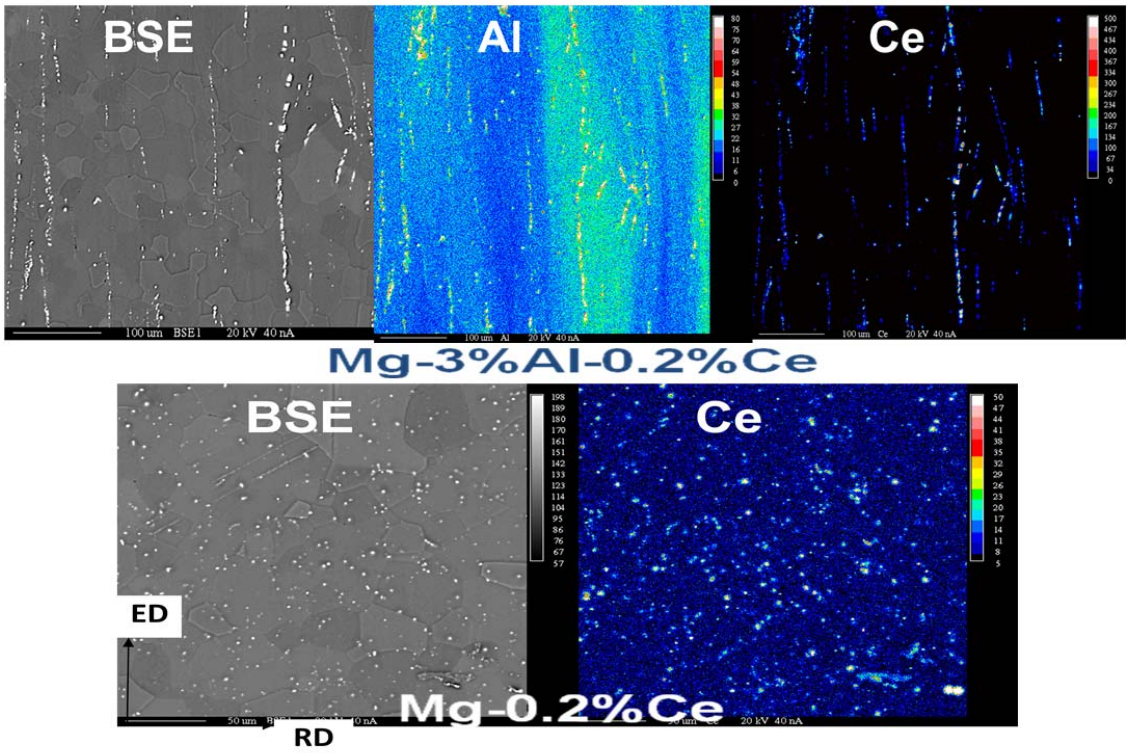

Fig. 5 Microprobe analysis showing the backscattered images and the element distribution maps for Mg-3Al-0.2Ce alloy and Mg-0.2 Ce alloy.

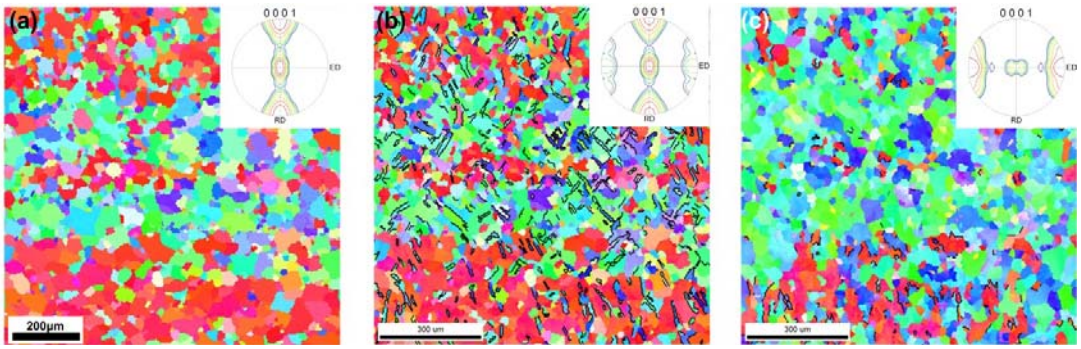

Fig.6 IPF and PF maps illustrating the microstructure and texture evolution of AZ31 tube compressed at room temperature to true strain of: (a) 0.01 (b)0.09 (C) 0.18 and the max intensity of texture is 9.8, 8.4 and 13.9 respectively.